applied sciences

MDPI

Article

An Impedance Sensor in Detection of Immunoglobulin G with Interdigitated Electrodes on Flexible Substrate

Kai Jin [1], Ping Zhao [1], Wenhui Fang [1], Yingjiao Zhai [1], Siyi Hu [2], Hanbin Ma [2] and Jinhua Li [1,*]

[1] International Joint Research Center for Nanophotonics and Biophotonics, School of Science, Changchun University of Science and Technology, Changchun 130022, China; 2017100052@mails.cust.edu.cn (K.J.); 2018100045@mails.cust.edu.cn (P.Z.); whfang@cust.edu.cn (W.F.); zhaiyingjiao0613@cust.edu.cn (Y.Z.)

[2] CAS Key Laboratory of Bio-medical Diagnostics, Suzhou Institute of Biomedical Engineering and Technology, Chinese Academy of Sciences, No. 88 Keling Road, Suzhou 215163, China; husiyi@sibet.ac.cn (S.H.); mahb@sibet.ac.cn (H.M.)

* Correspondence: lijh@cust.edu.cn

Received: 26 April 2020; Accepted: 3 June 2020; Published: 10 June 2020

Abstract: Immunoassay plays an important role in the early screening and diagnosis of diseases. The use of electrochemical methods to realize the label-free, specific and rapid detection of antigens has attracted extensive attention from researchers. In this study, we realized the function of immunosensing and detection by lithography, the interdigitated gold electrode on the polyethylene naphthalate (PEN) membrane. Then, the gold electrode was biofunctionalized and the characterization was verified by atomic force microscopy, which was finally for the detection of mice IgG. This immunosensor has a low detection limit, with a broad linear detection range of 0.01–10 ng/mL. The results show that the electrochemical impedance sensor made of metal electrodes based on PEN flexible materials is suitable for immunoassay experiments. If this method could be proved by further studies, broad application prospects can be seen in routine immunoassays.

Keywords: electrochemical impedance spectroscopy (EIS); immunosensor; flexible electrodes

1. Introduction

Immunodiagnosis is a method to detect various diseases, based on the specific immune response between antigen and antibody [1,2]. Based on different labeling signals, various immunodiagnosis methods are derived. The immunodiagnostic methods include: enzyme-linked immunosorbent assay (ELISA) [3], immunofluorescence technology, radioimmunoassay (RIA), immunocolloid gold labeling (ICS), chemiluminescence immunoassay (CLIA) [4,5], etc. At present, CLIA and ELISA are widely used, especially in clinical diagnosis and experimental research [6]. They have become the mainstream of immunodiagnostic technology and have a particularly important position in modern medicine. The traditional immunoassay methods in these laboratories are not suitable for rapid on-site testing, due to the long sample preparation time and the need for laboratory personnel with professional background. The electrochemical immunosensor provide the possibilities for label-free detection, detecting electrical signals instead of optical signals. They have been widely applied in biological detections at different scales, including but not limited to, organs, tissues, cells and biomolecules. Therefore, the electrochemical immunoassay has attracted extensive attention because of its detection specificity, simple operation, and small size [7–9].

Electrochemical impedance spectroscopy (EIS) is a non-destructive steady-state technique that is capable of probing the relaxation phenomena over a range of frequencies [9]. It is widely adopted to analyze electrode process dynamics and clarify corrosion mechanisms [10,11]. The electrochemical

impedance biosensor is an analysis device that converts biological signals into electrical impedance signals [12–14]. It analyzes the changes of resistance and capacitance signals on the electrode surface to observe the process of the adsorption and interaction of biomolecules on the electrode surface ranging over enzymes, proteins, DNA, bacteria [10,15], etc. However, most current electrochemical impedance sensors are based on rigid, non-deformable substrates, resulting in that [16–18], sensors can hardly fit with the measured object faced with complicated test environments such as three-dimensional and bendable objects, thus, leading to measurement errors. The situation above limits the wider applications of the device in the field of biosensing detection [19,20]. Therefore, in order to better adapt to the test environment and reduce the measurement errors, flexible electrodes, with excellent performance, is desperately needed [19,21].

In this paper, we designed a novel 3 × 3 interdigital electrode array (with minimum electrode spacing of 20 μm) on the flexible and sensitive micro-immunosensor, which was fabricated by photolithography on flexible PEN film. The process flow chart of the device can be found in the supplementary file Figure S1. Using this system, we detected Phosphate Buffer Saline PBS of different concentrations and IgG of low concentration, moreover, a relatively wide linear detection interval of 0.01–10 ng/mL is obtained, which verified the feasibility of flexible PEN -based electrode for immunoassay. In further research, the system can be applied in complex environments such as three-dimensional biological tissues and can detect multiple proteins simultaneously for disease diagnosis.

2. Experimental Section

2.1. Materials

11-Mercaptoundecanoicacid (11-MUA, 98%),1-ethyl-3-carbodiimide hydrochloride (EDC, 99%), N-hydroxysuccinimide (NHS, 98%), bovine serum albumin (BSA), $K_3[Fe(CN)_6]$ (99%) and $K_4[Fe(CN)_6]$ (98.5–102.0%) were purchased from Sigma-Aldrich. Mouse Immunoglobulins G (IgG), goat anti-Mouse IgG (Anti-IgG) antibody were purchased from Beijing Biodragon Immunotechnologies Co., Ltd. (Beijing, China). Phosphate buffer saline (1×) (PBS, pH 7.2) was obtained from HyClone. Deionized water (DI) (18.2 MΩ*cm) from a Millipore water purification system was used to prepare all buffer solutions.

2.2. Design and Processing Test Electrodes

Figure 1 shows a system block diagram of a biosensor, including a physical diagram of the sensor and a schematic diagram of an impedance test. Flexible electrodes were fabricated on polyethylene naphthalate (PEN) by photolithography. Cr/Au (20/80 nm layer) were deposited on the surface of PEN and patterned by a dry etching process. The physical image is shown in Figure 1a. The minimum electrode spacing is 20 μm, the relative effective area of the interdigitated electrode is 5.628 mm^2, and the relative effective length is 139.6 mm, as shown in Figure 1d. In the field of flexible electronics, the mechanical strength of the PEN material has been demonstrated by our previous work and other scientists [22,23]. as shown in the right figure of Figure 1d. As shown in Figure 1b, the Poly Methyl Methacrylatemethacrylic Acid (PMMA) sheet, with a thickness of 2 mm, was cut into a 9-hole structure consistent with the electrode structure by a laser cutter and used as a sample cell. Its hole diameter is 6 mm, which equals the size of a standard 96-well plate. PMMA and flexible electrodes are bonded together by ultraviolet (UV) glue for later testing.

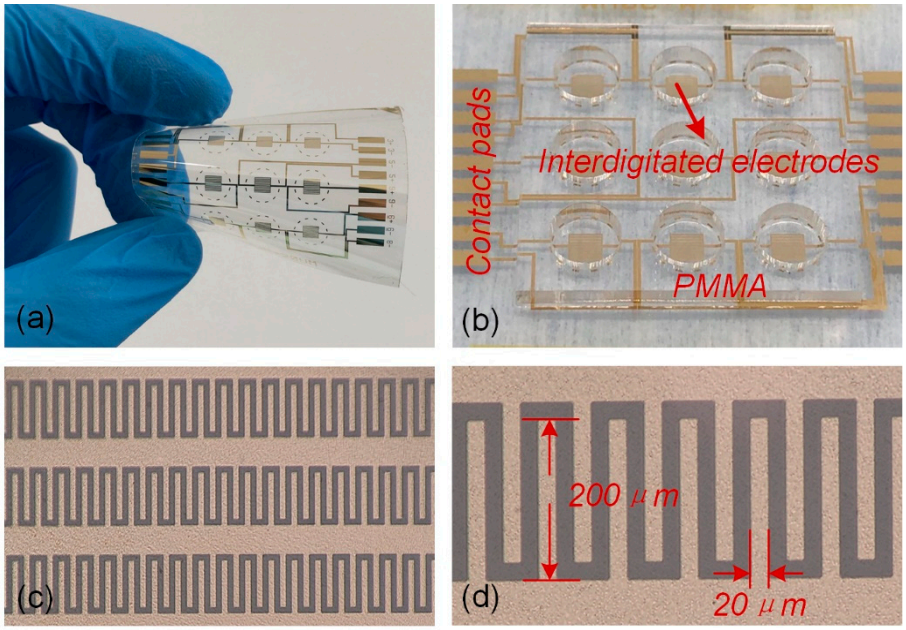

Figure 1. (**a**) Photographs of fabricating gold interdigitated electrodes on flexible PEN. (**b**) Physical picture of experimental test device; (**c**,**d**) Electrode local dimension diagram.

2.3. Verification Test of Electrode Detection Function

The experiement involved diluting the 1×PBS solution with DI water in equal proportions to obtain PBS sample solutions with 20 different concentrations. The electrode system was used to test sample solutions of different concentrations, and three parallel experiments were set up for each concentration.

Here, we control the curvature of the channel by changing the distance between the two measuring pads of the PEN electrode and conduct an impedance test on the 0.1×PBS solution.

2.4. Fabrication Process of Immunosensor

Here we fixed goat anti-mouse IgG to the surface of the gold electrode using standard biological functionalization steps. The electrode was washed 2–3 times with absolute ethanol solution and dried with nitrogen before the experiment. First, 11-MUA diluted to 2 mM with absolute ethanol was added to the sample cell for 1.5 h to form a self-assembling monolayer (SAM) layer on the surface of the electrode. Then carefully rinsed with alcohol to remove unbound SAM molecules. Second, in order to activate the SAM layer, a mixed solution of EDC (50 mM) and NHS (50 mM) was added to the sample cell for 20 min. Next, the electrodes were sequentially washed with DI water and PBS, then dried with nitrogen. A goat anti-mouse IgG solution at a concentration of 25 μg/mL was injected into the sample cell and incubated for 2 h. Finally, the electrode was immersed in PBS, containing 100 mM ethanolamine for 1 h at room temperature, to block the nonspecific binding sites, then washed twice with PBS and DI water.

2.5. Measurement and Apparatus

All impedance tests in this work were performed on a Gamry Interface 1010E electrochemical workstation. In the electrode verification experiment, the sample is directly dropped on the electrode for testing, and the test frequency is from 10 Hz to 1 MHz with an amplitude of 5 mV. In the immunoassay, all impedance measurements were performed in the presence of a 5 mM $[Fe(CN)_6]^{3-/4-}$ (1:1) mixture as a redox probe in PBS (pH 7.4). The test frequency range is 0.1 Hz to 1 MHz, and the amplitude is 5 mV. Record all Bode plots and Nyquist plots.

3. Results and Discussion

3.1. System Verification Experiment

The work of impedance measurement is based on the arrangement of bipolar electrodes. We input a small interference signal to the test system. The signal is transmitted from one electrode to another through the medium between the two electrodes, and finally, the signal is read through the electrochemical workstation. Figure 1a shows the physical diagram of the flexible interdigitated electrode array obtained by the photolithography process, Figure 1b shows the physical diagram of the experimental test device, Figure 1c,d show the partial dimensions of the interdigital electrode. Prior to performing the immunoassay experiment, as shown in the electrode schematic diagram of Figure 1b, three test areas were selected from the 3 × 3 interdigital electrode array test area. Three test areas were evaluated using 20 different PBS solutions. Figure 2a,b show the Bode plots (the relationship between impedance and phase and frequency) recorded in 5 PBS solutions of different concentrations. It can be seen that in the high frequency region (10 kHz–100 kHz), the impedance exhibits a pure resistance characteristic, which is mainly related to the difference in ion concentration in PBS solution. The impedance value decreases with increasing concentration. This relationship can be expressed by the following equation:

$$\rho = K * 1/n. \quad (1)$$

In the above formula, ρ is the resistivity of the liquid, n is the concentration of the liquid (usually proportional to the ion concentration), and K is constant when the temperature of the liquid is constant. The recorded EIS measurement data can be fitted by an equivalent circuit. The fitted line is represented by the solid line in Figure 2a,b. Here, the fitted curve and the measured data remain highly coincident. The fitting circuit is shown in the sub-graph of Figure 2a. This is a typical equivalent circuit [14], where the capacitor C_1 is the solution capacitor, the resistor Rs is the test resistor, and the capacitor C_2 is the polarization capacitor, and there is a constant phase element (CPE). By fitting all the data, the test resistance Rs is extracted. Figure 2c shows the trend of R_s with solution samples of 20 different concentrations. The data plotted are the average of 20 measurements in different wells, and standard deviations (STD) are plotted as error bars. The data shows that the sensor exhibits high uniformity between different wells in the experiment of solution concentration sensing. When the PBS concentration is in the range of 0.01×–0.0001×, the relationship between R_s and concentration is highly linear, and the error bars of the concentration fitting data R_s are very small thus can be almost ignored, so the linear detection interval of the sensor for the solution concentration is 0.01×–0.0001× (0.1 mM–0.001 mM). Figure 2d shows the comparison between this PBS concentration measurement experiment and the previous work. It can be seen, in the figure, that the oblique line of this test is almost equivalent to shifting to the upper left compared to the previous time, which indicates that the sensitivity is almost unchanged. In this case, the sensor can maintain the test sensitivity at lower concentrations. The sensitivity difference between this experiment and the previous work is 4% [10]. The reason for the above phenomenon is that the miniature interdigital electrode used in this electrode has an electrode gap of 20 microns. The electrode gap and the contact area between the electrode and the liquid are different. The above proves that this kind of electrode made with flexible PEN has good uniformity and sensitivity.

In order to further prove that the electrodes remain of good sensing function after bending, we conducted a verification experiment of the detection function under different bending angles. See supplementary documents Figures S3 and S4. Further sensor detection applications provide new possibilities.

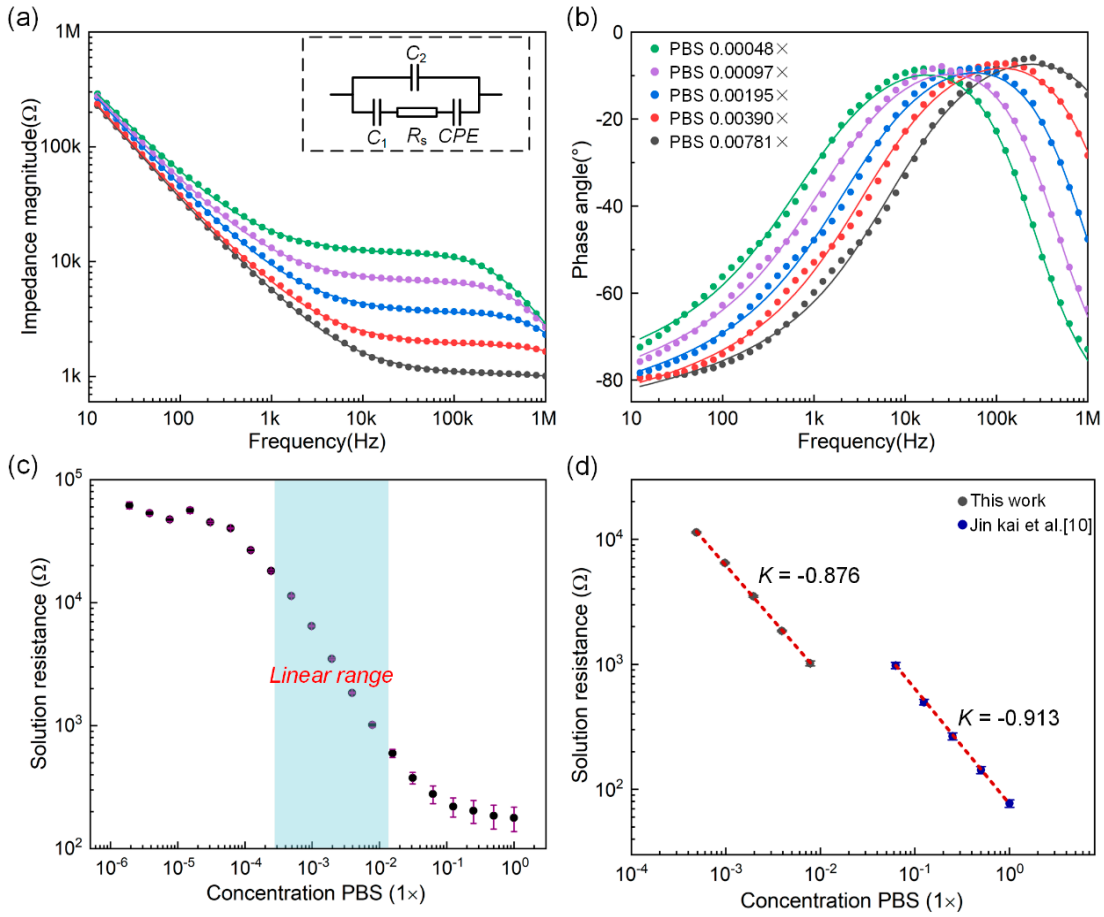

Figure 2. (**a**,**b**) show the impedance measurements and fitting values of PBS solutions of five different concentrations within the linear interval; (**c**) the relationship between the equivalent resistance Rs and the concentration; (**d**) compares the relationship between PBS concentration and equivalent resistance with previous work.

3.2. Gold Electrodes Biofunctionalization and Characterization

The schematic diagram of the biological functionalization step of immobilizing the antibody on the flexible Au electrode is shown in Figure 3. First, by incubating 11-MUA, a stable self-assembled monolayer (SAM) was formed on the surface of the gold electrode. Since 11-MUA has a long alkyl chain, it can provide van der Waals force between the molecules, forming a solid, close-packed two-dimensional (2D) molecular array [24,25]. As part of the conventional standard process for modifying the SAM layer on gold surface, this method has been adopted by most researchers for its convenience and practicality. The concentration of 11-MUA used in this study has been confirmed in most literatures, and is capable of immunoassay [18,26,27]. Then the NHS/EDC is added to activate the SAM layer before the amino group of the protein molecules were stably bounded to the activated SAM layer. Finally, ethanolamine molecules are used to block the sites of unbounded protein molecules to avoid non-specific binding during antigen detection.

In order to confirm the formation of the self-assembled monolayer (SAM) on the surface of the gold electrode, we conducted Atomic Force Microscope (AFM) tests on the gold electrode surface before and after biofunctionalization (shown in Supplementary Figure S2).

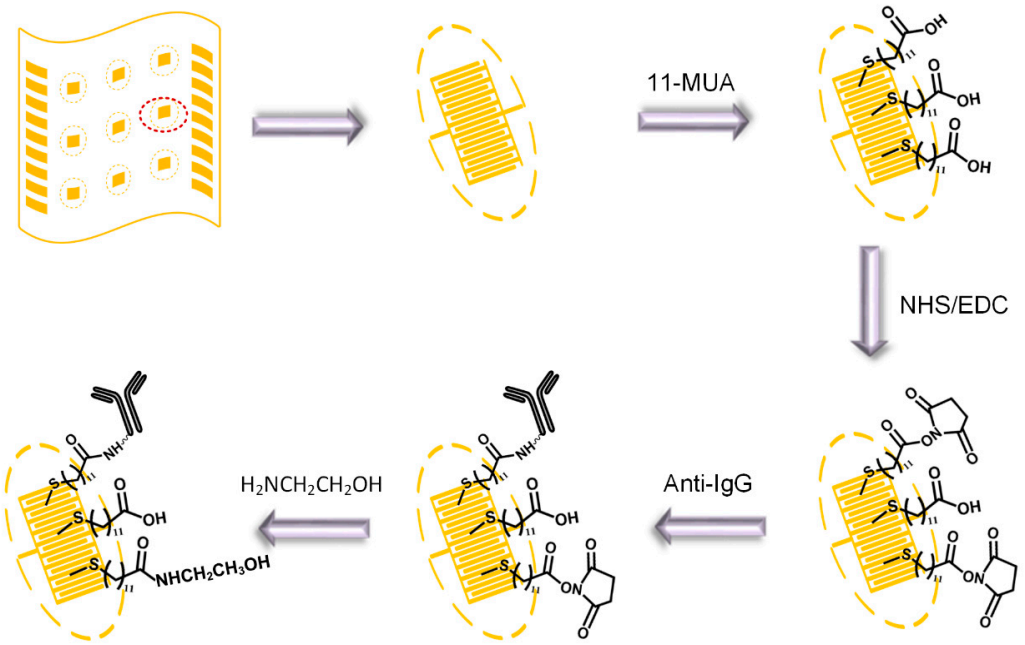

Figure 3. Shows the biofunctionalization steps of the interdigitated gold electrode.

3.3. Analysis of Equivalent Circuit of Immune Sensing

Figure 4a shows the equivalent circuit model of impedance data fitting. The dashed line and solid line in Figure 4b represent the Nyquist plot of the measured impedance and the comparison of the fitted data according to the equivalent circuit. The two curves are highly coincident and have a good fitting effect. This circuit consists of five circuit elements: Solution resistance R_s, constant phase elements CPE_1 and CPE_2, constant resistance R_a and charge transfer resistance R_{ct}. It can be understood here that we divide the surface of the electrode into an internal SAM layer and external biomolecules (antigen and antibody). The internal part is composed of a constant resistance and a constant phase element CPE_2, and the external part is composed of a charge transfer resistance R_{ct} and Another constant-phase original CPE_1, and R_s represents the resistance of the electrolyte solution [28].

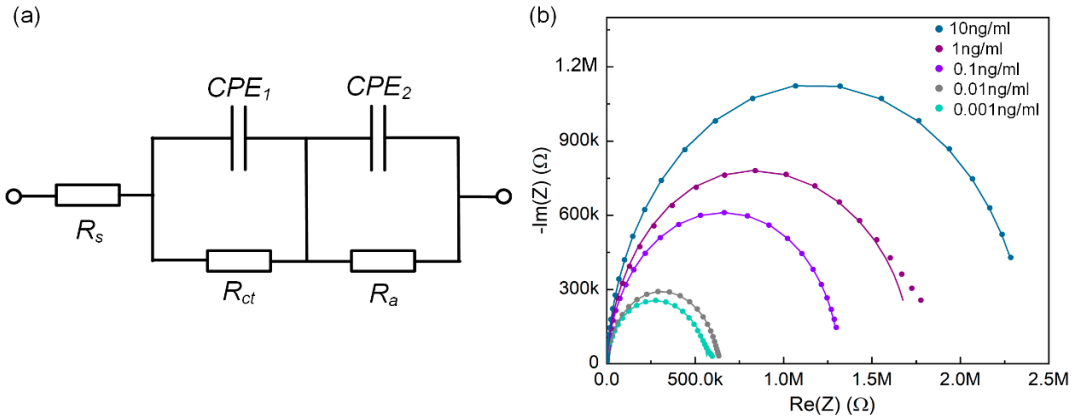

Figure 4. (**a**) the equivalent circuit model of the immune analysis in this paper; (**b**) Nyquist plots of actual measured and fitted values of impedance after incubation of different concentrations of IgG.

In the immunoassay experiment, Faraday impedance was measured using $[Fe(CN)_6]^{3-/4-}$ as the REDOX probe, and R_{ct} stands for the charge transfer resistance of the REDOX probe $[Fe(CN)_6]^{3-/4-}$. The formation of biomolecular membrane on the electrode surface would block the transfer of $[Fe(CN)_6]^{3-/4-}$ charge, resulting in the increase of the R_{ct} of the charge transfer resistance. Since the ability of the

antibody on the sensor surface to capture the antigen is related to the concentration of the antigen itself, we can judge the concentration of the antigen by monitoring the change in charge transfer resistance of the reduction probe $[Fe(CN)_6]^{3-/4-}$ before, and after, the immune response.

3.4. Impedance-Based Immunoassay

In order to test the sensing performance of the sensor, IgG solutions of five different concentrations: 0.001 ng, 0.01 ng, 0.1 ng, 1 ng, and 10 ng were sequentially incubated on the biofunctional electrode for 30 min. After each incubation, the electrode was washed with 1×PBS and dried with a nitrogen gun. Then the redox solution, containing $[Fe(CN)_6]^{3-/4-}$ was added into the acrylic tank and the EIS spectrum was read. When immunoassay was performed, the Nyquist diagram showed an obvious semicircle. The range of R_{ct} was between 500 k and 2.5 M, indicating the immune response of IgG on the electrode, which strongly limited the charge transfer between $[Fe(CN)\ 6]^{3-/4-}$. In addition, the range of R_{ct} was smaller than the previously reported range of 3 M–7 M. The reason for this difference is that our cross-finger electrode area (5.628 mm^2) is larger than the previously reported electrode area (0.5 mm^2) [18]. Figure 4b shows the changes in the Nyquist plot at different concentrations. We have intuitively observed that, the diameter of the Nyquist diagram semicircle has gradually increased with the rise of incubation antigen IgG concentration, revealing the increase of impedance. As described in Section 3.3, we extracted the charge transfer resistance R_{ct} for each test. Here, we consider the blocking step as the zero point, that is, $\Delta R = R_{ct}$ (IgG) − R_{ct} (Blocking). This standardized ΔR can truly reflect the IgG concentration.

Figure 5 shows the relationship between normalized resistance ΔR and concentration C. in the range of 0.01 ng–10 ng/mL. With higher IgG concentration, the logarithm of ΔR and concentration presents a linear regression with a high determination coefficient $R_2 = 0.991$. When the concentration drops to 1 pg/mL, the impedance data cannot read correctly, indicating that the concentration is below the lowest detection line of the system. It can be seen in the Figure that the linear detection interval of the biosensor is 0.01 ng/mL–10 ng/mL, and the linear regression equation in this interval is:

$$\Delta R = 567.79 \log_{10}[C] + 1243.2, \quad (2)$$

The minimum detection limit is about 0.01 ng/mL. The above shows that our miniature interdigital gold electrode based on PEN flexible material is suitable for the manufacture of high-performance immunosensors.

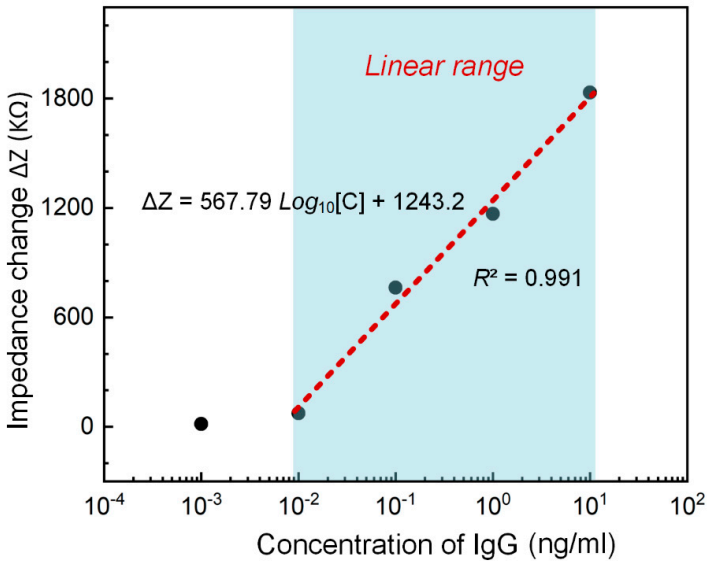

Figure 5. The response trend line of the immunosensor.

4. Conclusions

In this paper, a flexible PEN-based interdigitated gold electrode was used to achieve fast and label-free immunosensing, while the dense interdigitated electrodes structure made the sensor more sensitive. Impedance uniformity tests of PBS solutions of 20 different concentrations were used to evaluate the uniformity and sensitivity of flexible interdigital electrodes. The gold surface was subsequently modified by several chemical methods, and later physical characterization verified that the gold electrode was successfully modified by antigen molecules. Finally, EIS tests were performed on IgG solutions of five different concentrations, and the antigen concentrations were inferred from the charge transfer resistance changes of the redox probe $[Fe(CN)_6]^{3-/4-}$ before and after the immune response. The minimum detection limit is about 0.01 ng/mL, according to the experimental result. In this paper, immunosensors array based on flexible PEN showed excellent performance. In the future, flexible substrate can play a role in various complex three-dimensional test environments and will have great potential in the development of biosensors.

Supplementary Materials: The following are available online at http://www.mdpi.com/2076-3417/10/11/4012/s1, Figure S1: System process flow and assembly diagram. Figure S2. AFM test results before and after interdigital gold electrode biofunctionalization. Figure S3. Physical picture of flexible electrode in three different bending forms. Figure S4. Under three electrode shapes with different degrees of bending, test the impedance and frequency change curve of 0.1 × PBS solution.

Author Contributions: Conceptualization, J.L., H.M.; methodology, K.J., J.L.; validation, K.J.; writing—original draft preparation, K.J.; formal analysis, K.J.; investigation, P.Z., Y.Z., W.F.; review and editing, S.H., J.L.; All authors have read and agreed to the published version of the manuscript.

Funding: This research was funded by the "111" Project of China (D17017), the National Natural Science Foundation of China (21703017, 11604024), the Advance Recearch Project of Equipment (6140414020102), the Developing Project of Science and Technology of Jilin Province (20180519017JH, 20190201181JC), the International Science and Technology Cooperation Project of Jilin Province (20190701029GH).

Acknowledgments: We'd like to express gratitude to the Micro-nano processing platform of Suzhou institute of biomedical engineering and technology, Chinese academy of sciences, for offering facilities and necessary conditions for the device processing.

Conflicts of Interest: The authors declare that they have no conflict of interest.

References

1. Pai, M.; Riley, L.W.; Colford, J.M. Interferon-γ assays in the immunodiagnosis of tuberculosis: A systematic review. *Lancet Infect. Dis.* **2004**, *4*, 761–776. [CrossRef]
2. Schachter, J. Immunodiagnosis of sexually transmitted disease. *Yale J. Biol. Med.* **1985**, *58*, 443. [PubMed]
3. Rockstroh, A.; Barzon, L.; Kumbukgolla, W.; Su, H.X.; Lizarazo, E.; Vincenti-Gonzalez, M.F.; Tami, A.; Ornelas, A.M.M.; Aguiar, R.S.; Cadar, D.J. Dengue Virus IgM Serotyping by ELISA with Recombinant Mutant Envelope Proteins. *Emerg. Infect. Dis.* **2019**, *25*, 112. [CrossRef] [PubMed]
4. Ehsani, M.; Chaichi, M.J.; Hosseini, S.N. Comparison of CuO nanoparticle and CuO/MWCNT nanocomposite for amplification of chemiluminescence immunoassay for detection of the hepatitis B surface antigen in biological samples. *Sens. Actuators B Chem.* **2017**, *247*, 319–328. [CrossRef]
5. Liu, R.; Zhang, S.; Wei, C.; Xing, Z.; Zhang, S.; Zhang, X. Metal stable isotope tagging: Renaissance of radioimmunoassay for multiplex and absolute quantification of biomolecules. *Acc. Chem. Res.* **2016**, *49*, 775–783. [CrossRef] [PubMed]
6. Chen, D.; Zhang, Y.; Xu, Y.; Shen, T.; Cheng, G.; Huang, B.; Ruan, X.; Wang, C. Comparison of chemiluminescence immunoassay, enzyme-linked immunosorbent assay and passive agglutination for diagnosis of Mycoplasma pneumoniae infection. *Therap. Clin. Risk Manag.* **2018**, *14*, 1091. [CrossRef] [PubMed]
7. Ricci, F.; Volpe, G.; Micheli, L.; Palleschi, G. A review on novel developments and applications of immunosensors in food analysis. *Anal. Chim. Acta* **2007**, *605*, 111–129. [CrossRef] [PubMed]
8. Shankaran, D.R.; Gobi, K.V.; Miura, N. Recent advancements in surface plasmon resonance immunosensors for detection of small molecules of biomedical, food and environmental interest. *Sens. Actuators B Chem.* **2007**, *121*, 158–177. [CrossRef]

9. Pejcic, B.; De Marco, R. Impedance spectroscopy: Over 35 years of electrochemical sensor optimization. *Electrochim. Acta* **2006**, *51*, 6217–6229. [CrossRef]
10. Jin, K.; Hu, S.; Su, Y.; Yang, C.; Li, J.; Ma, H. Disposable impedance-based immunosensor array with direct-laser writing platform. *Anal. Chim. Acta* **2019**, *1067*, 48–55. [CrossRef]
11. Lisdat, F.; Schäfer, D. The use of electrochemical impedance spectroscopy for biosensing. *Anal. Bioanal. Chem.* **2008**, *391*, 1555. [CrossRef] [PubMed]
12. Chang, B.-Y.; Park, S.-M. Electrochemical impedance spectroscopy. *Annu. Rev. Anal. Chem.* **2010**, *3*, 207–229. [CrossRef]
13. Varshney, M.; Li, Y. Interdigitated array microelectrodes based impedance biosensors for detection of bacterial cells. *Biosens. Bioelectron.* **2009**, *24*, 2951–2960. [CrossRef] [PubMed]
14. Li, X.; Yu, M.; Chen, Z.; Lin, X.; Qi, W. A sensor for detection of carcinoembryonic antigen based on the polyaniline-Au nanoparticles and gap-based interdigitated electrode. *Sens. Actuators B Chem.* **2017**, *239*, 874–882. [CrossRef]
15. Drummond, T.G.; Hill, M.G.; Barton, J.K. Electrochemical DNA sensors. *Nat. Biotechnol.* **2003**, *21*, 1192–1199. [CrossRef] [PubMed]
16. Ma, H.; Su, Y.; Nathan, A. Cell constant studies of bipolar and tetrapolar electrode systems for impedance measurement. *Sens. Actuators B Chem.* **2015**, *221*, 1264–1270. [CrossRef]
17. Sharma, R.; Deacon, S.E.; Nowak, D.; George, S.E.; Wälti, C.J.B. Label-free electrochemical impedance biosensor to detect human interleukin–8 in serum with sub-fg/mL sensitivity. *Biosens. Bioelectron.* **2016**, *80*, 607–613. [CrossRef] [PubMed]
18. Shin, S.R.; Zhang, Y.S.; Kim, D.-J.; Manbohi, A.; Avci, H.; Silvestri, A.; Aleman, J.; Hu, N.; Kilic, T.; Keung, W. Aptamer-based microfluidic electrochemical biosensor for monitoring cell-secreted trace cardiac biomarkers. *Anal. Chem.* **2016**, *88*, 10019–10027. [CrossRef] [PubMed]
19. Gao, W.; Emaminejad, S.; Nyein, H.Y.Y.; Challa, S.; Javey, A. Fully integrated wearable sensor arrays for multiplexed in situ perspiration analysis. *Nature* **2016**, *529*, 509–514. [CrossRef] [PubMed]
20. Chung, S.; Lee, T. Towards flexible CMOS circuits. *Nat. Nanotechnol.* **2020**, *15*, 11–12. [CrossRef] [PubMed]
21. Gong, X.X.; Fei, G.T.; Fu, W.B.; Fang, M.; Gao, X.D.; Zhong, B.N.; De Zhang, L. Flexible strain sensor with high performance based on PANI/PDMS films. *Org. Electron.* **2017**, *47*, 51–56. [CrossRef]
22. Feng, L.; Jiang, C.; Ma, H.; Guo, X.; Nathan, A. All ink-jet printed low-voltage organic field-effect transistors on flexible substrate. *Org. Electron.* **2016**, *38*, 186–192. [CrossRef]
23. Grego, S.; Lewis, J.; Vick, E.; Temple, D. A method to evaluate mechanical performance of thin transparent films for flexible displays. *Thin Solid Films* **2007**, *515*, 4745–4752. [CrossRef]
24. Nelles, G.; Schönherr, H.; Jaschke, M.; Wolf, H.; Schaub, M.; Küther, J.; Tremel, W.; Bamberg, E.; Ringsdorf, H.; Butt, H.-J. Two-Dimensional Structure of Disulfides and Thiols on Gold (111). *Langmuir* **1998**, *14*, 808–815. [CrossRef]
25. Choi, H.-G.; Min, J.; Lee, W.H.; Choi, J.-W. Adsorption behavior and photoelectric response characteristics of bacteriorhodopsin thin films fabricated by self-assembly technique. *Colloids Surf. B* **2002**, *23*, 327–337. [CrossRef]
26. Wan, J.; Ai, J.; Zhang, Y.; Geng, X.; Gao, Q.; Cheng, Z. Signal-off impedimetric immunosensor for the detection of Escherichia coli O157: H7. *Sci. Rep.* **2016**, *6*, 19806. [CrossRef] [PubMed]
27. Fu, Y.; Yuan, R.; Tang, D.; Chai, Y.; Xu, L. Study on the immobilization of anti-IgG on Au-colloid modified gold electrode via potentiometric immunosensor, cyclic voltammetry, and electrochemical impedance techniques. *Colloid. Surface. B* **2005**, *40*, 61–66. [CrossRef] [PubMed]
28. Ohno, R.; Ohnuki, H.; Wang, H.; Yokoyama, T.; Endo, H.; Tsuya, D.; Izumi, M. Electrochemical impedance spectroscopy biosensor with interdigitated electrode for detection of human immunoglobulin A. *Biosens. Bioelectron.* **2013**, *40*, 422–426 All authors have read and agreed to the published version of the manuscript. [CrossRef] [PubMed]